Sorting Nexin 9 facilitates podocin endocytosis in the injured podocyte

Yu Sasaki[1], Teruo Hidaka[1], Takashi Ueno[2], Miyuki Akiba-Takagi[1], Juan Alejandro Oliva Trejo[1,3], Takuto Seki[1,3], Yoshiko Nagai-Hosoe[1], Eriko Tanaka[1,4], Satoshi Horikoshi[1], Yasuhiko Tomino[1], Yusuke Suzuki[1] and Katsuhiko Asanuma[1,3,*]

1 Division of Nephrology, Department of Internal Medicine, Juntendo University Faculty of Medicine, Tokyo, Japan

2 Laboratory of Proteomics and Biomolecular Science, Research Support Center, Juntendo University Graduate School of Medicine, Tokyo, Japan

3 Medical Innovation Center, TMK project, Graduate School of Medicine, Kyoto University, Kyoto, Japan

4 Department of Pediatrics and Developmental Biology, Graduate School of Medicine, Tokyo Medical and Dental University, Tokyo, Japan

Correspondence: *Katsuhiko Asanuma MD, PhD

Medical Innovation Center, TMK Project, Kyoto University Graduate School of Medicine,

53 Shogoin Kawaharacho, Sakyo-ku, Kyoto 606-8507, Japan

Tel: +81-75-366-7437

E-mail: asanuma@tmk.med.kyoto-u.ac.jp

Conflicts of Interest Statement:

None of the authors has a direct conflict of interest relevant to this study.

Beyond the study contents, Katsuhiko Asanuma has received research funding from Mitsubishi Tanabe Pharmaceutical Corporation.

The irreversibility of glomerulosclerotic changes depends on the degree of podocyte injury. We have previously demonstrated the endocytic translocation of podocin to the subcellular area in severely injured podocytes and found that this process is the primary disease trigger. Here we identified the protein sorting nexin 9 (SNX9) as a novel facilitator of podocin endocytosis in a yeast two-hybrid analysis. SNX9 is involved in clathrin-mediated endocytosis, actin rearrangement and vesicle transport regulation. Our results revealed and confirmed that SNX9 interacts with podocin exclusively through the Bin–Amphiphysin–Rvs (BAR) domain of SNX9. Immunofluorescence staining revealed the expression of SNX9 in response to podocyte adriamycin-induced injury both *in vitro* and *in vivo*. Finally, an analysis of human glomerular disease biopsy samples demonstrated strong SNX9 expression and co-localization with podocin in samples representative of severe podocyte injury, such as IgA nephropathy with poor prognosis, membranous nephropathy and focal segmental glomerulosclerosis. In conclusion, we identified SNX9 as a facilitator of podocin endocytosis in severe podocyte injury and demonstrated the expression of SNX9 in the podocytes of both nephropathy model mice and human patients with irreversible glomerular disease.

Introduction

Kidney podocytes, which are highly specialized, terminally differentiated epithelial cells located outside of the glomerular basement membrane, serve as a final barrier to urinary protein loss[1]. Continuous injury to the podocytes induces irreversible podocyte loss and glomerulosclerosis development, leading to chronic renal failure[2]. As the number of patients with end-stage renal disease is growing worldwide[3], it is very important to prevent or attenuate podocyte injury and thus protect the kidneys from chronic renal failure; in this context, elucidating the pathogenesis of podocyte injury is urgently needed.

Several proteins play key roles in the maintenance of podocyte integrity. In particular, slit-diaphragm proteins, such as nephrin, podocin and CD2AP, were found to be critical in the prevention of proteinuria because the mutation and inactivation of these proteins led to severe proteinuria and consequent chronic renal failure[4]. Podocin is expressed at the slit diaphragm, where it is thought to act as an intracellular scaffold protein by assembling slit-diaphragm components in lipid raft-associated microdomains[4,5]. Indeed, Boute et al. were the first to demonstrate a causative link between mutations in *NPHS2*, which encodes podocin, and childhood nephrotic syndrome[6]. In addition, NPHS2 was found to be the most frequently affected gene associated with steroid-resistant nephrotic syndrome[7], and dysregulated podocin intracellular trafficking was observed in several diseases associated with *NPHS2* mutations[8].

Endocytosis serves as a portal; specifically, this process involves the formation of vesicles for the internalization and retrieval of plasma membrane components or transmembrane receptors. Endocytic trafficking can be divided into two main pathways; the classic clathrin-mediated endocytic pathway and the non-classic clathrin-independent pathway[9]. To date, a great deal of work has focused on clathrin-mediated endocytosis (CME), leading to an increasing understanding of the mechanisms by which the proteins involved in this process recruit cargo into developing clathrin-coated pits and subsequently form clathrin-coated vesicles[10]. Although CME is certainly an extremely important endocytic mechanism that accounts for a large proportion of endocytic events, an ever-expanding array of cargo has been shown to undergo endocytosis in a clathrin-independent

manner[11].

Recent findings from studies on genetic mouse models of disease, as well as human genetic mutations that result in the loss of integrity of the glomerular filtration barrier, suggest a critical role for endocytosis in podocyte biology[12]. This is because in podocytes, the endocytic process plays a fundamental role in the development and maintenance of the glomerular filtration barrier. Thus, the loss of key molecular machinery results in defective actin regulation, faulty slit-diaphragm maintenance and increases the uptake of lipoproteins, or integrins, which might have deleterious effects on podocyte health[13].

Previously, our group has discovered a difference in the immunostaining patterns of podocin and synaptopodin, normally co-located in the foot process, in both a rat model of puromycin aminonucleoside nephrosis (PAN) and patients with IgA nephropathy[14]. In this previous study, localization of podocin shifted from the slit diaphragm to the podocyte cytoplasm in the context of severe podocyte injury, suggesting a role for endocytosis in glomerular health.

Here we describe a further novel finding that the protein sorting nexin 9 (SNX9) interacts with podocin in podocytes. SNX9 is specifically involved in endocytosis and also participates in actin rearrangement and regulates various stages of vesicle transport[15,16]. We demonstrate that SNX9 is strongly expressed and co-localizes with podocin in both kidneys from adriamycin (ADR)-injected mice and kidney biopsy samples from human patients with glomerular diseases leading to glomerulosclerosis. Our evidence indicates that SNX9 plays a role in podocin endocytosis and might help to advance our understanding of podocyte injury.

Results

The Bin–Amphiphysin–Rvs (BAR) domain of SNX9 interacts with podocin.

To identify a protein that would trigger podocin endocytosis, we conducted a yeast two-hybrid screening using the C-terminal fragment of podocin as bait. We identified SNX9, a member of the sorting nexin family of proteins that is widely expressed and plays a role in endocytosis, as a novel podocin-interacting protein. Next, we conducted co-immunoprecipitation assays to confirm the interaction between podocin and SNX9 using lysates of FLAG-podocin- and GFP-SNX9-overexpressing cells and confirmed an interaction between podocin and SNX9 *in vitro*. We used HEK293T cells as podocytes which show relatively low level of transfection efficiency, typical ranging from 10% to 20% for cells grown under permissive conditions[17], making it difficult to overexpress gene. To map the podocin binding site(s) in SNX9, we tested the abilities of various truncated GFP-SNX9 constructs[18] to co-precipitate with FLAG-podocin (Fig. 1a, b); results show that both GFP SNX9-BAR and SNX9-PX-BAR co-precipitate with FLAG-podocin, while SNX9-ΔBAR and SNX9-ΔPX-BAR do not interact with podocin, and no SNX9 binding was observed with a FLAG control (Fig. 1b). To further demonstrate that podocin can directly bind to SNX9, we performed GST pull-down assays with purified recombinant proteins according to our previously published protocols[19]. Purified GST-SNX9, not GST alone, binds to purified FLAG-podocin (Fig. 1c), and podocin was subsequently recognized as a band with an apparent molecular mass of 42 kDa using Western blot analysis. Additional higher molecular weights were also detected, suggesting the presence of podocin oligomers[20]. To further confirm the interaction between podocin and SNX9, endogenous proteins were immunoprecipitated from ADR-treated cultured podocytes using anti-podocin and anti-SNX9 antibodies. Anti-SNX9 antibody precipitated SNX9 and coprecipitated podocin. Conversely, anti-podocin antibody precipitated podocin and coprecipitated SNX9 (Fig. 1d). However, anti-GFP antibody did not precipitate SNX9 or podocin. Therefore, these results could prove the interaction between SNX9 and podocin via the BAR domain of SNX9 in injured podocytes.

To delineate the functional relevance of the SNX9–podocin interaction, we conducted

co-transfection studies of COS7 cells. First, we tested whether SNX9 would interact with podocin in COS7 cells and found that following transient transfection, GFP-SNX9 did indeed co-localize with FLAG-podocin. Next, to confirm the results of our co-immunoprecipitation assay, we co-transfected cells with truncated GFP-SNX9 mutants and FLAG-podocin. Again, GFP-SNX9-BAR co-localized with FLAG-podocin. In contrast, when cells were co-transfected with FLAG-podocin and a GFP-SNX9 mutant lacking the BAR domain, we observed little co-localization (Fig. 2). These data confirm the results of our co-immunoprecipitation assay and verify that SNX9 interacts with podocin via the SNX9 BAR domain.

Kidneys from ADR-injected mice exhibit high levels of co-localized SNX9 and podocin.

In a previous study, we demonstrated translocation of podocin to the cytoplasm via the endocytosis pathway in injured podocytes[14]. Here, we investigated the potential association of SNX9 with the endocytic translocation of podocin to the cytoplasm in injured podocytes. Using immunofluorescence staining to detect SNX9 expression in kidney samples from normal and ADR-injected mice (Fig. 3), we observed weak SNX9 expression and little co-localization with podocin in the normal mouse kidney (day zero), in contrast to a significant increase in SNX9 expression in the podocyte cytoplasm on days seven and 14 after ADR injection. We further noted that despite a decrease in podocin expression after ADR injection, as described previously[21], the SNX9 and podocin immunofluorescent signals were merged after ADR injection, especially in the podocyte cytoplasm.

SNX9 facilitates the translocation of podocin in injured human podocytes.

To evaluate SNX9 expression *in vitro*, we subjected non-treated and ADR-treated cultured human podocytes to immunofluorescence staining (Fig. 4a). Non-treated cultured podocytes showed very little SNX9 expression; in contrast, SNX9 expression was significantly increased in podocytes after ADR treatment. Notably, SNX9 expression increased in a dose-dependent manner. Additionally, we confirmed the co-localization of SNX9 with podocin in podocytes following ADR treatment, which

159 further confirmed the SNX9–podocin interaction.

160 To study the localization of SNX9 and podocin in ADR-treated podocytes, we performed
161 subcellular fractionation using OptiPrep gradient centrifugation. Podocin remained in fractions 11–
162 13 after ADR treatment. However, SNX9 appeared *de novo* in fractions 9–13 and was distributed in
163 the same fractions where podocin was predominant (Fig. 4b). To study the localization of SNX9 and
164 podocin in ADR-treated podocytes, we used subcellular fractionation with OptiPrep gradient
165 centrifugation and found that SNX9 distributed in the same fractions where podocin were
166 predominant (Fig. 4b). To investigate the potential association of SNX9 with the endocytic
167 translocation of podocin to the cytoplasm in injured podocytes, To investigate the role of SNX9 in
168 injured podocytes, we studied the loss-of-function of SNX9 in ADR-treated podocytes. A decrease in
169 SNX9 expression was found in SNX9 siRNA-transfected podocytes compared with that in
170 non-transfected podocytes (Fig. 4c). SNX9 siRNA-transfected podocytes after ADR treatment
171 exhibited obvious membranous and moderate cytoplasmic expression of podocin, whereas
172 non-transfected podocytes after ADR treatment exhibited strong cytoplasmic and little membranous
173 expression.

174

175 **SNX9 co-localizes with endosomal markers in transfected COS7 cells.**

176 To confirm the involvement of SNX9 in endocytosis, COS7 cells were transfected with GFP-SNX9
177 (Fig. 5) and subsequently co-stained with EEA1 and Rab5 (early endosomal compartment marker).
178 Notably, co-localization of SNX9 dots with EEA1 dots was detected in merged figures obtained
179 under high magnification. Furthermore, results show that co-localization of SNX9 with Rab5 was
180 more pronounced.

181

182 **SNX9 is detectable in human kidneys affected by IgA nephropathy, membranous nephropathy**
183 **and focal segmental glomerulosclerosis.**

184 To assess SNX9 expression in human kidney glomeruli, we subjected human kidney biopsy
185 specimens to immunofluorescence staining (see Methods). Normal human kidney tissues show

moderate SNX9 glomerular staining as shown in The Human Protein Atlas; http://www.proteinatlas.org/. SNX9 expression and co-localization with podocin were significantly higher in specimens from patients with IgA nephropathy with poor prognosis (IgAN-poor), membranous nephropathy (MN) and focal segmental glomerulosclerosis (FSGS); these specimens are associated with severe podocyte injury compared with those from controls, patients with minimal change nephrotic syndrome (MCNS) and patients with IgA nephropathy with a good prognosis (IgAN-good; Fig. 6).

Discussion

In this study, we identified the protein SNX9 as a novel interaction partner of podocin in podocytes. We detected strong SNX9 expression and co-localization with podocin in ADR-injected mice and samples from human patients with severe glomerular diseases such as IgAN-poor, MN and FSGS, suggesting a pivotal role for SNX9 in podocin endocytosis under pathological conditions.

Sorting nexins have roles in diverse processes such as endocytosis, endosomal sorting and signaling[22, 23]. Given their fundamental natures, these proteins are associated with diseases in which endosomal function is adversely perturbed, such as Alzheimer's disease and pathogenic infection[24,25]. In this study, SNX9 was found to interact with podocin via its BAR domain; this domain enables the formation of a crescent-shaped homodimer, senses and generates positive membrane curvature and induces membrane tubulation[26]. Furthermore, membrane tubulation via polymeric BAR domain assembly is thought to be regulated by lipid binding[27]. As podocin is a lipid mitochondria protein[17] that recruits cholesterol to organize the lipid microenvironment of associated ion channel complexes[28], podocin is thought to have an affinity for the BAR domain, and these structures share a similar polymerizing function. Our data are consistent both with these inferred roles and their functions.

Recent findings have suggested a critical role for endocytosis in podocyte biology, with a particular focus on nephrin[29,30,31]. However, very little is known about podocin endocytosis, and its precise mechanisms remain unclear. Nevertheless, Shono et al. have demonstrated that podocin co-localizes with the coxsackie virus and adenovirus receptor (CAR) at the tight junctions between foot processes in PAN rat kidneys and that podocin facilitates the coalescence of lipid rafts containing CAR and thus promotes dynamic cytoskeletal arrangements[32]. Moreover, podocin and CAR exhibit a diffuse punctate pattern throughout the cytoplasm in COS-7 cells co-transfected with both proteins. In contrast, however, Godel et al. demonstrated that a fraction of podocin resides in the CD63/LAMP3-positive late endosomal compartment and has limited co-localized with EEA1 in transiently co-transfected HeLa cells[33]. We recently reported considerable co-localization of both

podocin and nephrin with Rab7 and LAMP1 in podocyte-specific cathepsin D knock-out mice (CD^{pdKO}), compared with control mice[34], suggesting that podocin and nephrin are mainly localized in the late endosomes and lysosomes of CD^{pdKO} mouse podocyte cell bodies. Further, electron microscopic examination revealed that cytoplasmic podocin was localized in granular osmiophilic deposits (GRODs).

One previous report has demonstrated that podocin trafficking depends on the raft-mediated, non-classic, clathrin-independent endocytic pathway[33]. Intriguingly, the podocin-related protein flotillin-1 defines a clathrin-independent endocytic pathway[35], suggesting that podocin not only assembles members of the slit diaphragm, but also orchestrates their internalization via a self-defined pathway[33]. Our group demonstrated the co-localization of podocin with Rab5 in PAN rats, a model of glomerular sclerosis development, indicating that podocin interacts with the CME pathway. We have also previously clarified[15,16] that SNX9 is involved in CME via immunofluorescent analysis of transfected COS7 cells. Specifically, transiently expressed GFP-SNX9 is co-localized with both EEA1 and Rab5, indicating a role for SNX9 in CME. Consistent with our earlier findings[14], this study demonstrates the involvement of SNX9 in severe podocyte injury and a potential role for this protein as a trigger of podocin endocytosis by CME.

Regarding podocyte endocytosis, Soda et al. reported massive proteinuria and kidney failure with histological features suggestive of FSGS in podocyte-specific dynamin-1 and 2 double knock-out mice[36]. This finding supports an important role for dynamin, which is essential to CME, in the maintenance of the renal permeability barrier[37]. Notably, SNX9, which binds directly to dynamin and stimulates dynamin assembly, also stimulates the basal GTPase activity of dynamin and thus potentiates assembly-stimulated GTPase activity on liposomes[39]. The SNX9-dependent recruitment of dynamin to the membrane is regulated by an interaction between SNX9 and aldolase[39]. In other words, SNX9 is required for efficient CME and regulates dynamin activity. In this study, SNX9 expression emerged in the setting of severe glomerular damage, indicating that SNX9 might facilitate podocin endocytosis by regulating dynamin in an attempt at protection from severe damage. Furthermore, ADR-treated SNX9 KD podocytes exhibited obvious membranous and moderate

cytoplasmic expression of podocin, whereas non-transfected cell exhibited strong cytoplasmic and little membranous expression. These data indicate that SNX9 is crucial and may facilitate podocin endocytosis in injured podocytes. As ADR induces cell death, it is difficult to obtain sufficient amount of ADR-treated cultured podocytes for western blot analysis. Although few cells survived after ADR treatment, it was possible to perform immunohistochemistry. Therefore, the cells were cultured with a stronger ADR treatment for immunohistochemistry. SNX9 may connect with podocin during the early phase of podocyte injury, as indicated by the subcellular fractionation of cultured human podocytes, and then recruit podocin to cytoplasm during the late phase of podocyte injury, as indicated by immunohistochemistry.

After endocytosis, cargo enters and is sorted in the early endosomes and is either recycled back to the plasma membrane or degraded in the late endosomes and lysosomes[9]. The destinies of slit-diaphragm proteins following endocytosis remains unclear, as cargo can be transferred from early to late endosomes followed by lysosomal degradation, the trans-Golgi network and recycling endosomes[13]. Podocin was found to be internalized with SNX9 in early endosomes, designated by EEA1 and Rab5, and co-localized with the late endosomal proteins Rab7 and LAMP1[34]. SNX9 might promote podocyte injury by degrading podocin in lysosomes, or prevent damage by recycling podocin back to the plasma membrane.

In conclusion, we have demonstrated the emergence of SNX9 expression and consequent internalization of podocin via endocytosis in an ADR-induced nephropathy model, as well as in samples from patients with IgA nephropathy with a poor prognosis, MN and FSGS. SNX9 immunostaining might indicate the degree of podocyte injury. Furthermore, SNX9 may be the key to understanding glomerular injury. Future studies involving SNX9 knockout and overexpression models might clarify the role of SNX9 in podocyte injury.

293

Methods

295 **Yeast two-hybrid screen**.

296 The C-terminus of human podocin (amino acids 268–383; GenBank accession number gi:
297 7657614) was cloned into the bait vector pGBKT7 (BD Biosciences Clontech, San Jose, CA) to
298 create a fusion protein with the GAL4 DNA binding domain; this was subsequently transformed into
299 the yeast strain AH109 as described previously[40]. Briefly, a pre-transformed human kidney
300 MATCHMAKER cDNA library was screened in accordance with the manufacturer's protocol
301 (MATCHMAKER TwoHybrid System 3; BD Biosciences Clontech). Prey plasmids were isolated,
302 sequenced and retransformed into AH109 cells in combination with the podocin bait construct, a
303 control plasmid (pGBKT7-lamin; BD Biosciences Clontech), or the empty bait vector pGBKT7 to
304 exclude false positives.

305

306 **Plasmid constructs**.

307 GFP-SNX9 was kindly provided by S. Lance MaCaulay[41], while GFP-SNX9-BAR,
308 GFP-SNX9-ΔBAR, GFP-SNX9-PXBAR and GFP-SNX9-ΔPXBAR were provided by Sunghoe
309 Chang[18], and podocin-containing plasmids were provided by K. Schwarz[20]. PCR products were
310 ligated into the FLAG 5a plasmid (Sigma-Aldrich, St. Louis, MO, USA), and all constructs were
311 verified by DNA sequencing.

312

313 **Cell culture and transfection**.

314 Conditionally immortalized human podocyte cells were a gift from Moin A. Saleem (Bristol Royal
315 Hospital for Children Bristol, Bristol, UK) and were cultured as previously described[42]. Transient
316 transfection of HEK293T and COS7 cells (ATCC) was performed using FuGene 6 Reagent (Roche,
317 Indianapolis, IN, USA) at a 1:3 DNA:Fugene ratio in accordance with the manufacturer's protocol.
318 GFP-fusion proteins in living cells were analysed using direct fluorescence microscopy.
319 For ADR-treatment evaluation, cultured podocytes were treated with 0.1–0.2 μg/ml of ADR in a

regular medium for 6 h. After treatment, podocytes were washed twice in the medium and then maintained in ADR-free medium for 48 h. As a control, cultured podocytes were treated with normal sterile saline for the same time period and similarly washed. For endogenous co-immunoprecipitation and subcellular fractionation from ADR-treated podocytes, cells were treated with 0.2 μg/ml of ADR in a regular medium for 6 h and then maintained in ADR-free medium for 48 h. Cultured podocytes transfected with control siRNA and SNX9 siRNA were treated with 0.25μg/ml of ADR in a regular medium for 9 h and then maintained in ADR-free medium for 48 h for immunohistochemistry.

To generate SNX9 KD podocytes, GIPZ lentiviral shRNA system (GE Dharmacon, CO, USA) was used according to the manufacturer's instructions. In brief, HEK293T cells were transfected with shRNA plasmid DNA containing GFP (GIPZ non-silencing lentiviral shRNA control as a control, V2LHS_114991 as SNX9 KD) to produce lentiviral particles. Differentiated cultured podocytes were transduced with the lentiviral particles.

Antibodies.

Monoclonal mouse Rab5 antibody (#50523; Abcam, Tokyo, Japan), rabbit polyclonal GFP antibody (GFP-Rb-Af2020; Frontier Institute, Ishikari, Hokkaido, Japan), mouse monoclonal FLAG antibody (F1804; Sigma-Aldrich), goat polyclonal EEA1 antibody (sc-6415; Santa Cruz Biotechnology, Dallas, TX, USA), goat polyclonal GST antibody (27-4577; GE Healthcare, Wauwatosa, WI, USA), Alexa Fluor 488-conjugated donkey anti-rabbit IgG antiserum, and Alexa Fluor 555-conjugated goat anti-mouse IgG antiserum (Invitrogen, Carlsbad, CA, USA) were purchased for immunohistochemistry and/or Western blot analysis. Polyclonal rabbit and guinea pig anti-podocin sera have been described previously[20].

Antibodies against calnexin (C4731; Sigma Aldrich, St. Louis, MO, USA), caveolin (ab2910; Abcam, Cambridge, UK), and LAMP1 (MAB4800; R&D Systems, Minneapolis, MN, USA) were purchased for subcellular fractionation. Antibody against the β subunit of mitochondrial F1F0-ATPase was prepared as described previously[43].

To generate antibodies against human SNX9, rabbits were immunized with a hemocyanin-conjugated peptide (single letter code, CFGHPQAYQGPATGDD) corresponding to the amino acids of human SNX9, and resulting antibodies were affinity-purified as described previously[45] (see Supplementary Fig. S1 online).

Western blotting and immunoprecipitation.

For co-immunoprecipitation of FLAG and GFP fusion proteins, HEK293T cells were grown on a 10-cm dish to approximately 60% confluence, co-transfected and harvested on ice after 48 h with 5 ml of 50 mM EDTA in phosphate-buffered saline (PBS). Cells were pelleted by centrifugation and washed twice with ice-cold PBS. For cell lysis, the pellet was re-suspended in 1 ml of immunoprecipitation buffer (IP; 50 mM Tris [pH 7.5], 150 mM NaCl, 1.0% Triton X100, protease and phosphatase inhibitors) and incubated on ice for 30 minutes. The cell lysate was cleared by centrifugation for five minutes. One millilitre of cell extract was incubated overnight with 50 µl of agarose beads coated with anti-FLAG-M2 antibody (Sigma-Aldrich) at 4°C. Beads were collected by centrifugation and washed three times with 1 ml of IP buffer for 30 min on a rotator. Bound proteins were eluted by boiling agarose beads in 50 µl of Laemmli buffer at 95°C for five minutes. Samples were resolved on SDS–polyacrylamide gels, which were then transferred to membranes, and blocked with 5% non-fat milk solution; these were subsequently incubated with the appropriate primary antibodies. Antibodies against FLAG (Sigma) and GFP (Frontier Institute) were used at a 1:1,000 dilution, and HRP-conjugated secondary antibodies (Promega, Madison, WI, USA) were used at a 1:10,000 dilution. Images were scanned using a C-Digit chemiluminescent Western blot scanner, and densitometry analysis was performed using Image Studio Digits software (LI-COR Biosciences, Lincoln, NE, USA). Endogenous co-immunoprecipitations of lysates from ADR-treated podocytes were performed as previously described[40] using the following polyclonal primary antibodies: anti-podocin, anti–SNX9 and anti-GFP (negative control).

GST-binding assays.

374 To study the competitive binding of SNX9 to podocin, GST pulldown studies using purified
375 recombinant proteins were performed as described previously[19]. In brief, FLAG-tagged proteins
376 were expressed in HEK293T cells and purified. A total of 1 μg of GST-SNX9 was immobilized on
377 GSH-agarose beads; the beads were washed five times in 1% Triton X100 in PBS, after which 1 μg
378 of purified FLAG-tagged podocin in 500 μl PBS was added. For competition studies, 0, 100, 500, or
379 1000 ng of purified FLAG-podocin were added. Reactions were incubated under rotation for 2 h at
380 4°C, after which the beads were washed five times in PBS. Proteins were eluted in 100 μl of sample
381 buffer and analysed by SDS-PAGE and immunoblotting. Antibodies against GST and FLAG were
382 used at a 1:1,000 dilution. HRP-conjugated secondary antibodies were used at a 1:10,000 dilution.
383
384 **Subcellular fractionation**.
385 OptiPrep was purchased from Nycomed Pharma (Oslo, Norway). Control human podocytes and
386 ADR-treated podocytes cultured in three 15-cm dishes were detached from dishes using cell scrapers,
387 suspended in PBS and pooled in 50-ml centrifugal tubes. The suspension was centrifuged at 700 × *g*
388 for 5 min. The cell pellet was suspended in 1-ml extraction buffer, containing 5 mM Tes-NaOH (pH
389 7.4), 0.3 M sucrose and protease inhibitor cocktail (Roche Diagnostics, Indianapolis, IN, USA), and
390 the cells were homogenized by passing the suspension through 26-gauge syringe (10 up–down
391 strokes). Homogenate was centrifuged at 700 × *g* for 5 min. The supernatant (post-nuclear
392 supernatant) was retained. The pellet was re-suspended in 1-ml extraction buffer, homogenized as
393 described above and re-centrifuged at 700 × *g* for 5 min. The pooled post-nuclear supernatant (1.6
394 ml) was loaded on 10-ml linear OptiPrep gradients (5%–25%) that had been prepared according to
395 the manufacturer's protocol and centrifuged at 150,000 × *g* for 3 h. Fractions of 0.9 ml were
396 collected from the bottom to the top. Aliquots of fractions were treated with SDS-PAGE sample
397 buffer, applied on 10% or 12.5% SDS-PAGE gels and electrophoresed. The separated polypeptides
398 were examined by western blot analyses using antibodies against LAMP1, β subunit of
399 mitochondrial F1F0-ATPase, calnexin, caveolin, podocin and SNX9.
400

Immunohistochemistry.

Differentiated podocytes and COS7 cells were cultured on collagen type I-coated cover slips. Differentiated podocytes were treated with ADR. Cells were fixed with 4% paraformaldehyde, permeabilised with 0.3% Triton and incubated with blocking solution (2% foetal calf serum [FCS], 2% bovine serum albumin [BSA], 0.2% fish gelatin in PBS) and primary and secondary antibodies. We used 4',6-diamidino-2-phenylindole (DAPI) as a nuclei marker. For the immunofluorescent staining of ADR mouse kidneys, the kidneys were fixed by perfusion of 4% paraformaldehyde and 20% sucrose in PBS. The fixed kidneys were frozen in optimal cutting temperature compound. Frozen 4-µm-thick sections sections were incubated with primary antibodies specific for SNX9 (anti-SNX9 rabbit polyclonal antibody), podocin (anti-podocin guinea pig polyclonal antibody) and developed with secondary antibodies. The human kidney specimens were fixed with cold acetone for five minutes and frozen 4-µm-thick sections were immunostained in the same manner as described for ADR mice. All images were captured using a confocal laser microscope (FV1000; Olympus, Tokyo, Japan).

Mouse Model.

Female BALB/c mice were purchased from a commercial vendor (Oriental Yeast Co., Ltd., Tokyo, Japan), and ADR nephropathy was induced as previously described[44]. In brief, ADR (doxorubicin hydrochloride; Wako, Osaka, Japan) diluted with 0.9% saline was injected into eight-week-old BALB/c mice via the tail vein at a dose of 11 mg/kg. Age-matched control mice were injected with an equal volume of PBS only. After anaesthesia with sodium pentobarbital (100 mg/kg BW; Dainippon Sumitomo Pharma, Osaka, Japan), mice were euthanized on days seven and 14 after the injection of ADR. All mice were housed under specific pathogen-free conditions in standard animal cages with free access to standard chow and drinking water. All animal handling and experiments were performed strictly in accordance with the recommendations of the guideline for the Care and Use of Laboratory Animals of the Juntendo University Faculty of Medicine. The experimental protocol was approved by the Animal Care and Use Committee of Juntendo University, Tokyo,

Japan.

Renal histology.

Mouse kidneys were fixed via perfusion with 4% paraformaldehyde and 20% sucrose in PBS. For the immunofluorescence study, fixed kidneys were frozen in optimal cutting temperature compound. Human kidney specimens were collected from kidney biopsies performed at Juntendo University Hospital, Tokyo, Japan. We analysed samples from two groups of patients with glomerular diseases; those with minor podocyte injuries and those with severe podocyte injuries. MCNS and IgAN-good prognosis cause minor podocyte injury, whereas IgAN-poor prognosis, MN and FSGS cause severe podocyte injury and consequent glomerulosclerosis. As human controls, we used biopsy samples from patients with minor glomerular abnormalities. We diagnosed and classified patients with IgA nephropathy according to the second guideline of IgA nephropathy[46]. All glomeruli in the stained areas of human kidney biopsy specimens were evaluated per patient. For immunostaining, each patient had two to six glomeruli, and six patients in each group were examined. The staining area was automatically quantified using Tissue Studio (Definiens, Munich, Germany)[47]. In brief, the glomerular area was carefully traced by hand and automatically measured. Custom-made image analysis algorithms were applied to the digital slides to automatically detect and quantify the staining areas. Behind a configured action stands a set of algorithms with defined parameters. The respective algorithms were automatically loaded. The staining area/glomerular area ratio was also calculated. This study was conducted according to the Declaration of Helsinki and was approved by the Institutional Review Board of Juntendo University Hospital. Informed consent was obtained from all patients.

Statistical analysis.

All statistical analyses were performed using GraphPad Prism version 6.0 for Windows (GraphPad Software Inc., San Diego, CA, USA). Data are presented as means ± standard errors of the means. Comparisons between groups were analysed using a one-way analysis of variance (ANOVA), or

455 Student's t-test. Differences with P values <0.05 were considered significant.

456 # References

457 1. Greka, A. & Mundel, P. Cell biology and pathology of podocytes. *Annu. Rev. Physiol.* **74,**
458 299-323 (2012).

459 2. Mundel, P. & Shankland, S. J. Podocyte biology and response to injury. *J. Am. Soc. Nephrol.* **13,**
460 3005-3015 (2002).

461 3. Jha, V. *et al*. Chronic kidney disease: global dimension and perspectives. *Lancet* **382,** 260-272
462 (2013).

463 4. Tryggvason, K., Patrakka, J. & Wartiovaara, J. Hereditary proteinuria syndromes and
464 mechanisms of proteinuria. *N. Engl. J. Med.* **354,** 1387-1401 (2006).

465 5. Huber, T. B. *et al.* Molecular basis of the functional podocin-nephrin complex: mutations in the
466 NPHS2 gene disrupt nephrin targeting to lipid raft microdomains. *Hum. Mol. Genet.* **12,**
467 3397-3405 (2003).

468 6. Boute, N. *et al.* NPHS2, encoding the glomerular protein podocin, is mutated in autosomal
469 recessive steroid-resistant nephrotic syndrome. *Nat. Genet.* **24,** 349-354 (2000).

470 7. Caridi, G., Trivelli, A., Sanna-Cherchi, S., Perfumo, F. & Ghiggeri, G. M. Familial forms of
471 nephrotic syndrome. *Pediatr. Nephrol.* **25,** 241-252 (2010).

472 8. Roselli, S., Moutkine, I., Gribouval, O., Benmerah, A. & Antignac, C. Plasma membrane
473 targeting of podocin through the classical exocytic pathway: effect of NPHS2 mutations. *Traffic*
474 **5,** 37-44 (2004).

475 9. Le Roy, C. & Wrana, J. L. Clathrin- and non-clathrin-mediated endocytic regulation of cell
476 signalling. *Nat. Rev. Mol. Cell Biol.* **6**, 112-126 (2005).

477 10. Doherty, G. J. & McMahon, H. T. Mechanisms of endocytosis. *Annu. Rev. Biochem.* **78,**
478 857-902 (2009).

479 11. Kirkham, M. & Parton, R. G. Clathrin-independent endocytosis: new insights into caveolae and
480 non-caveolar lipid raft carriers. *Biochim. Biophys. Acta* **1746,** 349-363 (2005).

481 12. Swiatecka-Urban, A. Membrane trafficking in podocyte health and disease. *Pediatr. Nephrol.* **28,**

1723-1737 (2013).

13. Inoue, K. & Ishibe, S. Podocyte endocytosis in the regulation of the glomerular filtration barrier. *Am. J. Physiol. Renal Physiol.* **309,** F398-405 (2015).
14. Fukuda, H. *et al.* Podocin is translocated to cytoplasm in puromycin aminonucleoside nephrosis rats and in poor-prognosis patients with IgA nephropathy. *Cell Tissue Res.* **360,** 391-400 (2015).
15. Yarar, D., Waterman-Storer, C. M. & Schmid, S. L. SNX9 couples actin assembly to phosphoinositide signals and is required for membrane remodelling during endocytosis. *Dev. Cell.* **13,** 43-56 (2007).
16. Lundmark, R. & Carlsson, S. R. SNX9 - a prelude to vesicle release. *J. Cell. Sci.* **122,** 5-11 (2009).
17. Shankland, S. J., Pippin, J. W., Reiser, J. & Mundel, P. Podocytes in culture: past, present, and future. *Kidney Int.* **72,** 26-36 (2007).
18. Shin, N. *et al.* Sorting nexin 9 interacts with dynamin 1 and N-WASP and coordinates synaptic vesicle endocytosis. *J. Biol. Chem.* **282,** 28939-28950 (2007).
19. Asanuma, K. *et al.* Synaptopodin orchestrates actin organization and cell motility via regulation of RhoA signalling. *Nat. Cell Biol.* **8,** 485-491 (2006).
20. Schwarz, K. *et al.* Podocin, a raft-associated component of the glomerular slit diaphragm, interacts with CD2AP and nephrin. *J. Clin. Invest.* **108,** 1621-1629 (2001).
21. Lydia, A. *et al.* Effects of 22-oxa-calcitriol on podocyte injury in adriamycin-induced nephrosis. *Am. J. Nephrol.* **35,** 58-68 (2012).
22. Carlton, J., Bujny, M., Rutherford, A. & Cullen, P. Sorting nexins--unifying trends and new perspectives. *Traffic* **6,** 75-82 (2005).
23. Seet, L. F. & Hong, W. The Phox (PX) domain proteins and membrane traffic. *Biochim. Biophys. Acta* **1761,** 878-896 (2006).
24. Rogaeva, E. *et al.* The neuronal sortilin-related receptor SORL1 is genetically associated with Alzheimer disease. *Nat. Genet.* **39,** 168-177 (2007).
25. Alto, N. M. *et al.* The type III effector EspF coordinates membrane trafficking by the

509 spatiotemporal activation of two eukaryotic signalling pathways. *J. Cell Biol.* **178,** 1265-1278
510 (2007).
511 26. Peter, B. J. *et al.* BAR domains as sensors of membrane curvature: the amphiphysin BAR
512 structure. *Science* **303,** 495-499 (2004).
513 27. Suetsugu, S. Higher-order assemblies of BAR domain proteins for shaping membranes.
514 *Microscopy (Oxf)* **65,** 201-210 (2016)
515 28. Huber, T. B., Schermer, B. & Benzing, T. Podocin organizes ion channel-lipid supercomplexes:
516 implications for mechanosensation at the slit diaphragm. *Nephron Exp. Nephrol.* **106,** e27-31
517 (2007).
518 29. Qin, X. S. *et al.* Phosphorylation of nephrin triggers its internalization by raft-mediated
519 endocytosis. *J. Am. Soc. Nephrol.* **20,** 2534-2545 (2009).
520 30. Tossidou, I. *et al.* CIN85/RukL is a novel binding partner of nephrin and podocin and mediates
521 slit diaphragm turnover in podocytes. *J. Biol. Chem.* **285,** 25285-25295 (2010).
522 31. Tossidou, I. *et al.* Podocytic PKC-alpha is regulated in murine and human diabetes and
523 mediates nephrin endocytosis. *PLoS One* **5,** e10185 (2010).
524 32. Shono, A. *et al.* Podocin participates in the assembly of tight junctions between foot processes
525 in nephrotic podocytes. *J. Am. Soc. Nephrol.* **18,** 2525-2533 (2007).
526 33. Godel, M., Ostendorf, B. N., Baumer, J., Weber, K. & Huber, T. B. A novel domain regulating
527 degradation of the glomerular slit diaphragm protein podocin in cell culture systems. *PLoS One*
528 **8,** e57078 (2013).
529 34. Yamamoto-Nonaka, K. *et al.* Cathepsin D in Podocytes Is Important in the Pathogenesis of
530 Proteinuria and CKD. *J. Am. Soc. Nephrol.* (2016). DOI:10.1681/ASN.2015040366
531 35. Glebov, O. O., Bright, N. A. & Nichols, B. J. Flotillin-1 defines a clathrin-independent
532 endocytic pathway in mammalian cells. *Nat. Cell Biol.* **8,** 46-54 (2006).
533 36. Soda, K. *et al.* Role of dynamin, synaptojanin, and endophilin in podocyte foot processes. *J.*
534 *Clin. Invest.* **122,** 4401-4411 (2012).
535 37. Sever, S. *et al.* Proteolytic processing of dynamin by cytoplasmic cathepsin L is a mechanism

for proteinuric kidney disease. *J. Clin. Invest.* **117,** 2095-2104 (2007).

38. Soulet, F., Yarar, D., Leonard, M. & Schmid, S. L. SNX9 regulates dynamin assembly and is required for efficient clathrin-mediated endocytosis. *Mol. Biol. Cell* **16,** 2058-2067 (2005).
39. Lundmark, R. & Carlsson, S. R. Regulated membrane recruitment of dynamin-2 mediated by sorting nexin 9. *J. Biol. Chem.* **279,** 42694-42702 (2004).
40. Asanuma, K. *et al.* Synaptopodin regulates the actin-bundling activity of alpha-actinin in an isoform-specific manner. *J. Clin. Invest.* **115,** 1188-1198 (2005).
41. MaCaulay, S. L. *et al.* Insulin stimulates movement of sorting nexin 9 between cellular compartments: a putative role mediating cell surface receptor expression and insulin action. *Biochem. J.* **376,** 123-134 (2003).
42. Saleem, M. A. *et al.* A conditionally immortalized human podocyte cell line demonstrating nephrin and podocin expression. *J. Am. Soc. Nephrol.* **13,** 630-638 (2002).
43. Kominami, E. *et al.* Specific storage of subunit c of mitochondrial ATP synthase in lysosomes of neuronal ceroid lipofuscinosis (Batten's disease). *J. Biochem.* **111,** 278-282 (1992).
44. Weins, A. *et al.* Differentiation- and stress-dependent nuclear cytoplasmic redistribution of myopodin, a novel actin-bundling protein. *J. Cell Biol.* **155,** 393-404 (2001).
45. Asanuma, K. *et al.* Dendrin location in podocytes is associated with disease progression in animal and human glomerulopathy. *Am. J. Nephrol.* **33,** 537-549 (2011).
46. Tomino, Y., Sakai, H. & Special Study Group (IgA Nephropathy) on Progressive Glomerular Disease. Clinical guidelines for immunoglobulin A (IgA) nephropathy in Japan, second version. *Clin. Exp. Nephrol.* 7, 93-97 (2003).
47. Peck, A. R. *et al.* Validation of tumor protein marker quantification by two independent automated immunofluorescence image analysis platforms. *Mod. Pathol.* (2016). DOI: 10.1038/modpathol.2016.112.

Acknowledgments

This work was supported, in part, by a Grant-in-Aid for Young Scientists (B) (26860648 to Y.N.-H) (15K19466 to M.A.-T) and by a Grant-in-Aid for Challenging Exploratory Research (26670431 to K.A).

Author Contributions

Study concept and design: Y.S., T.H. and K.A. Acquisition of data: Y.S., T.H., T.U., M. A.-T., J.A.O.T., T.S., Y.N.-H. and E.T. Analysis and interpretation of data: Y.S. Drafting of the manuscript: Y.S. Critical revision of the article for important intellectual content: T.H. and K.A. Funding: S.H. and Y.T. Study supervision: T.H. and K.A.

Additional Information

Supplementary information accompanies this paper at http://www.nature.com/srep.

Competing financial interests: The authors declare no competing financial interests.

How to cite this article:

589

590 # Figure Legends

591 **Figure 1. The BAR domain of SNX9 interacts with podocin.**

592 (**a**) Schematic diagram of SNX9 and its domain structure. (**b**) HEK293T cells were co-transfected
593 with FLAG-tagged podocin and GFP-SNX9 truncated mutants; the resulting immunoprecipitates
594 were immunoblotted with anti-GFP or anti-FLAG antibodies. The lower panel shows
595 immunoblotting of total cell lysates with anti-GFP antibody to verify the expression of each
596 truncated mutant. IP, immunoprecipitation. (**c**) GST–SNX9 fusion proteins, or GST alone, were
597 incubated, and each lysate was used for the pulldown assay. Complexes were resolved by
598 SDS-PAGE and immunoblotted with anti-FLAG antibodies. (d) Coimmunoprecipitation (Co-IP)
599 experiments showing that endogenous SNX9 interacts with podocin in ADR-treated cultured human
600 podocytes. Anti-SNX9 antibody precipitated SNX9 and coprecipitated podocin. Conversely,
601 anti-podocin antibody precipitated podocin and coprecipitated SNX9. Anti-GFP antibody did not
602 precipitate SNX9 and podocin.

603

604 **Figure 2. SNX9 co-localizes with podocin in transfected COS7 cells.**

605 Immunofluorescence analysis of transiently expressed GFP-tagged SNX9 truncated mutants (green),
606 FLAG-tagged podocin (red) and DAPI (blue) in wild-type COS7 cells. Boxes indicate higher
607 magnification areas presented on the right.

608

609 **Figure 3. Increased SNX9 expression and co-localization with podocin are detectable in mice**
610 **with ADR-induced nephrosis.**

611 Fluorescent micrographs of glomeruli from mice with ADR-induced nephrosis following
612 immunostaining for SNX9 (green) and podocin (red); merged areas are indicated in yellow. Boxes
613 indicate higher magnification areas presented on the right. Scale bar, 20 μm.

614

615 **Figure 4. Increased SNX9 expression and co-localization with podocin are detectable in the**

cytoplasm of ADR-treated WT podocytes, whereas SNX9 KD podocytes exhibit little cytoplasmic expression of podocin.

(**a**) Fluorescent micrographs of cultured human podocytes stained with SNX9 (green) and podocin (red) before and after ADR treatment (merged areas are in yellow). DAPI (blue) was used to indicate nuclei. Boxes indicate higher magnification areas presented in the lower panels. (**b**) Western blot analyses of the fractions from control podocytes or podocytes treated with ADR separated on linear OptiPrep gradients (5%–25%). Distributions of SNX9 and podocin, as well as marker proteins of plasma membrane (caveolin), endosome/lysosome (LAMP1), mitochondria (β subunit of F1F0-ATPase), and endoplasmic reticulum (calnexin), were examined by western blot analysis. (**c**) Cultured human podocytes were transfected with nonfunctional control siRNA (upper panel) or SNX9 siRNA (middle and lower panels). *Transfected cells,* as decided by *GFP* expression, are indicated by arrowheads. Upper panel: Fluorescent micrographs of control siRNA-transfected podocyte stained with SNX9 (red). Middle panel: Fluorescent micrographs of SNX9 siRNA-transfected podocyte with ADR treatment stained with SNX9 (red). Lower panel: Fluorescent micrographs of SNX9 siRNA-transfected podocyte with ADR treatment stained with podocin (red). DAPI (blue) was used to indicate nuclei. Boxes indicate higher-magnification areas presented on the right.

Figure 5. SNX9 localizes to the early endosomes in transfected COS7 cells.

Triplicate staining of transiently expressed GFP-tagged SNX9 (green), EEA1 (red, upper panel) or Rab5 (red, lower panel) and DAPI (blue). Boxes indicate higher magnification areas presented on the right.

Figure 6. SNX9 is strongly expressed and co-localizes with podocin in the context of severe podocyte injury related to human kidney disease.

(**a**) Fluorescent micrographs of glomeruli from human kidney biopsy specimens immunostained with SNX9 (green) and podocin (red); merged areas are in yellow. Kidney samples were diagnosed

643 pathologically.

644 (**b**) SNX9 intensity per glomerulus in human kidney biopsy specimens. More than two glomeruli per

645 patient and six patients per disease were examined, and the SNX9 staining area was automatically

646 quantified using Tissue Studio (Definiens, Munich, Germany; *P < 0.05 or **P < 0.001, one-way

647 ANOVA).

648 (**c**) Intensity of SNX9/podocin merged area per glomerulus in human kidney biopsy specimens.

649 More than two glomeruli per patient and six patients per disease were examined. The SNX9/podocin

650 merged area was automatically quantified using Tissue Studio (Definiens, Munich, Germany; *P <

651 0.05 or **P < 0.001, Student's t-test). Scale bar, 50 μm.

652

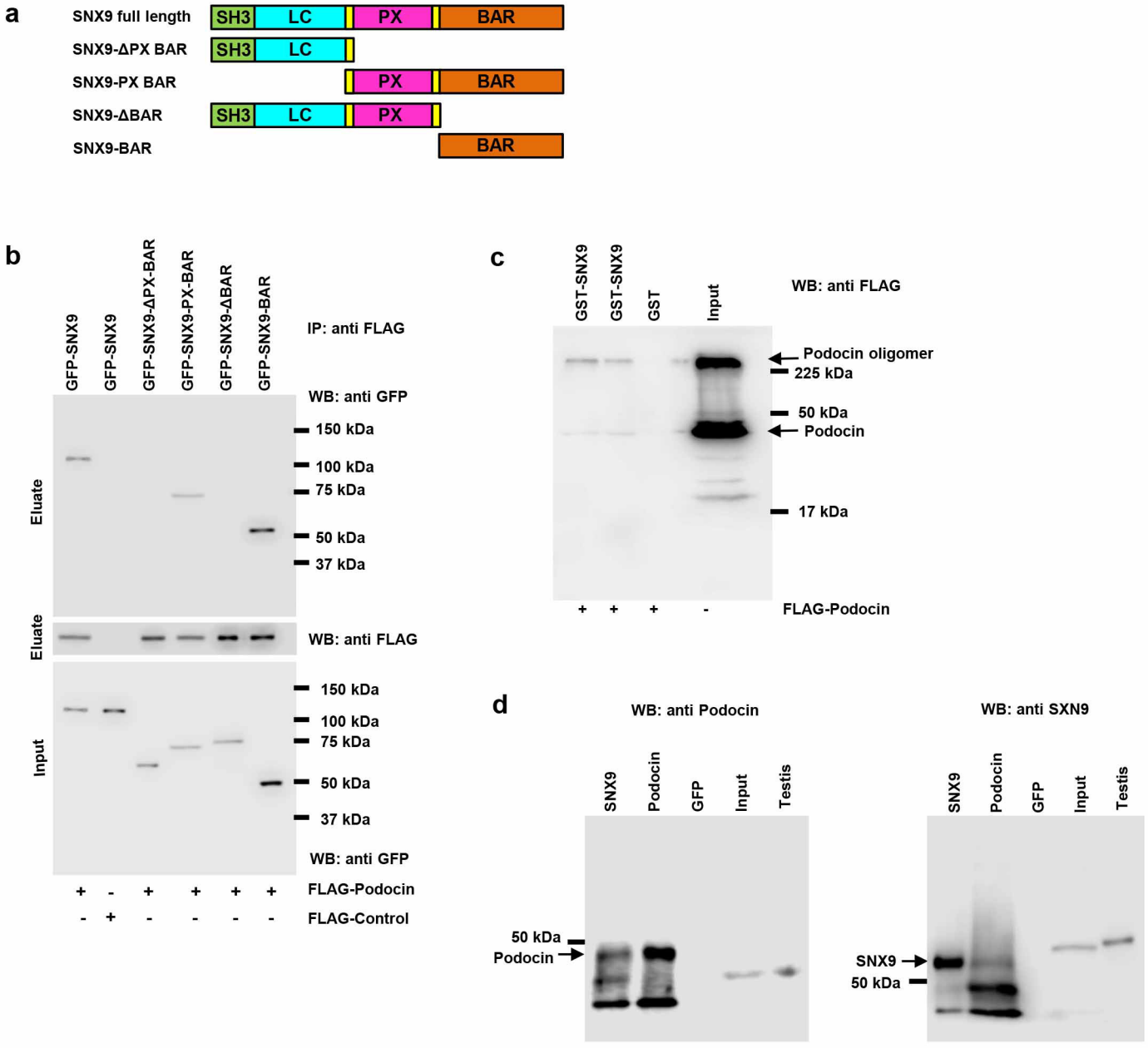
a
SNX9 full length
SH3
LC
PX
BAR
SNX9-ΔPX BAR
SNX9-PX BAR
SNX9-ΔBAR
SNX9-BAR
b
GFP-SNX9
GFP-SNX9
GFP-SNX9-ΔPX-BAR
GFP-SNX9-PX-BAR
GFP-SNX9-ΔBAR
GFP-SNX9-BAR
IP: anti FLAG
WB: anti GFP
150 kDa
100 kDa
75 kDa
50 kDa
37 kDa
Eluate
Eluate
WB: anti FLAG
Input
150 kDa
100 kDa
75 kDa
50 kDa
37 kDa
WB: anti GFP
+ - + + + + FLAG-Podocin
- + - - - - FLAG-Control
c
GST-SNX9
GST-SNX9
GST
Input
WB: anti FLAG
Podocin oligomer
225 kDa
50 kDa
Podocin
17 kDa
+ + + - FLAG-Podocin
d
WB: anti Podocin
SNX9
Podocin
GFP
Input
Testis
50 kDa
Podocin
WB: anti SXN9
SNX9
Podocin
GFP
Input
Testis
SNX9
50 kDa

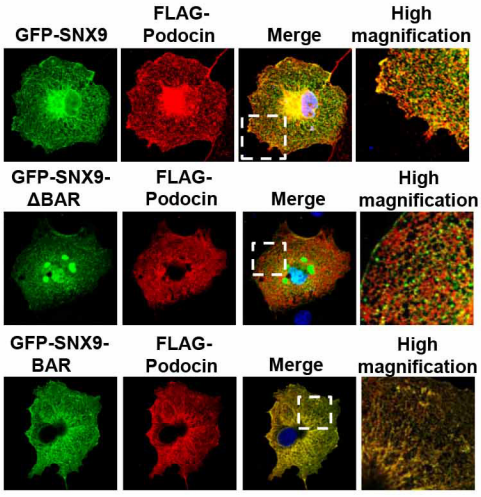
GFP-SNX9
FLAG-Podocin
Merge
High magnification
GFP-SNX9-ΔBAR
FLAG-Podocin
Merge
High magnification
GFP-SNX9-BAR
FLAG-Podocin
Merge
High magnification

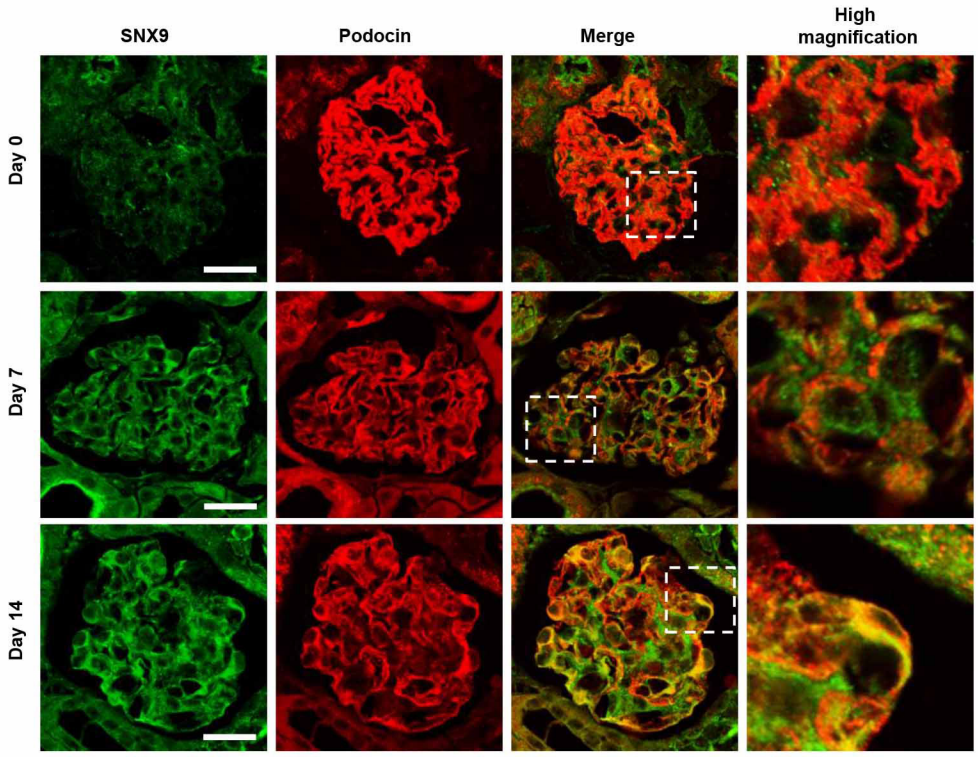
SNX9
Podocin
Merge
High magnification
Day 0
Day 7
Day 14

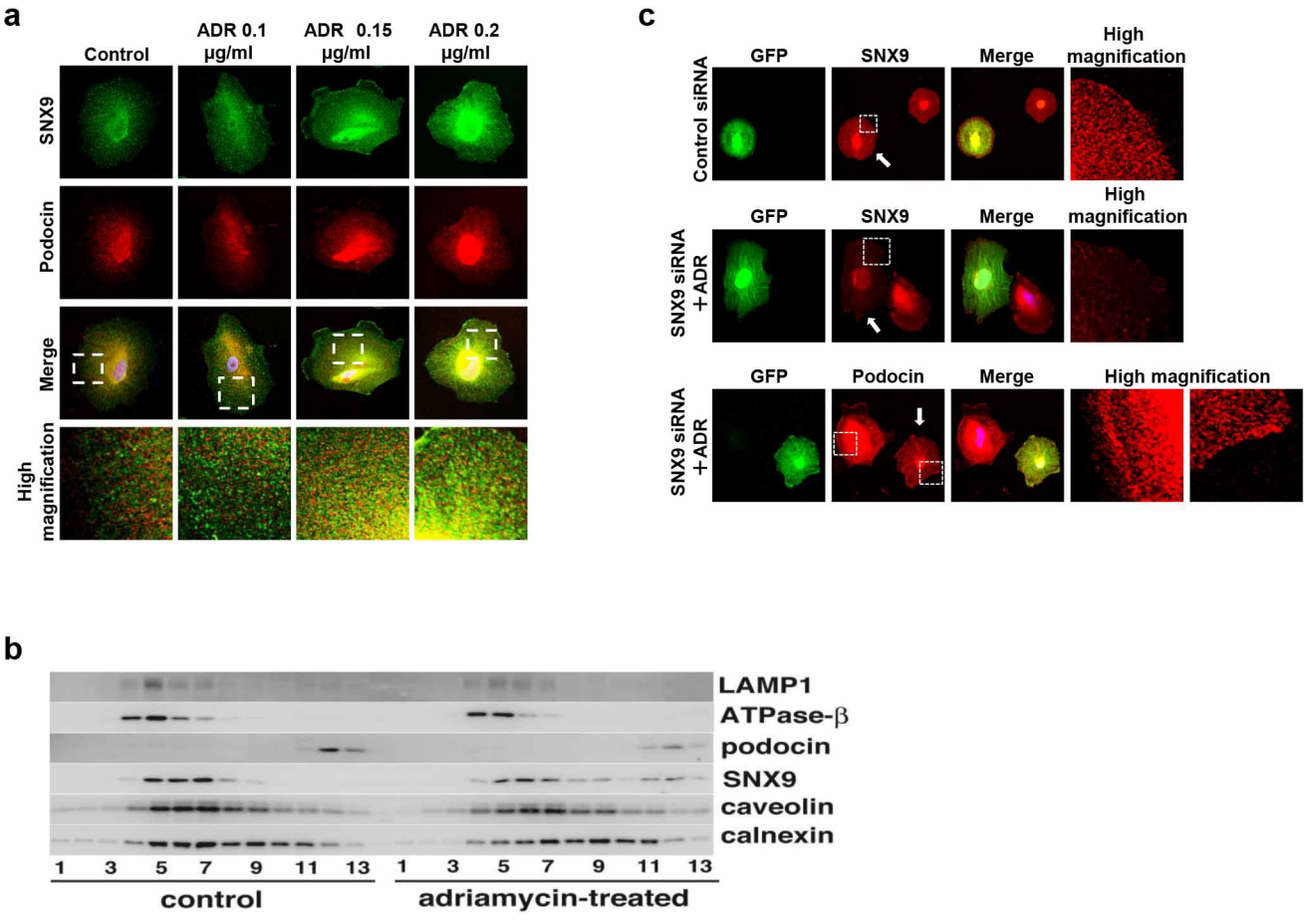
a
Control
ADR 0.1 μg/ml
ADR 0.15 μg/ml
ADR 0.2 μg/ml
SNX9
Podocin
Merge
High magnification
c
GFP
SNX9
Merge
High magnification
Control siRNA
SNX9 siRNA +ADR
Podocin
High magnification
b
LAMP1
ATPase-β
podocin
SNX9
caveolin
calnexin
1 3 5 7 9 11 13
control
adriamycin-treated

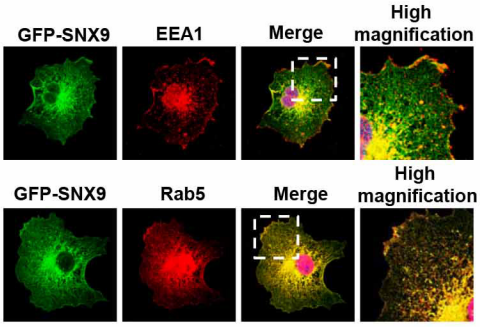
GFP-SNX9
EEA1
Merge
High magnification
GFP-SNX9
Rab5
Merge
High magnification

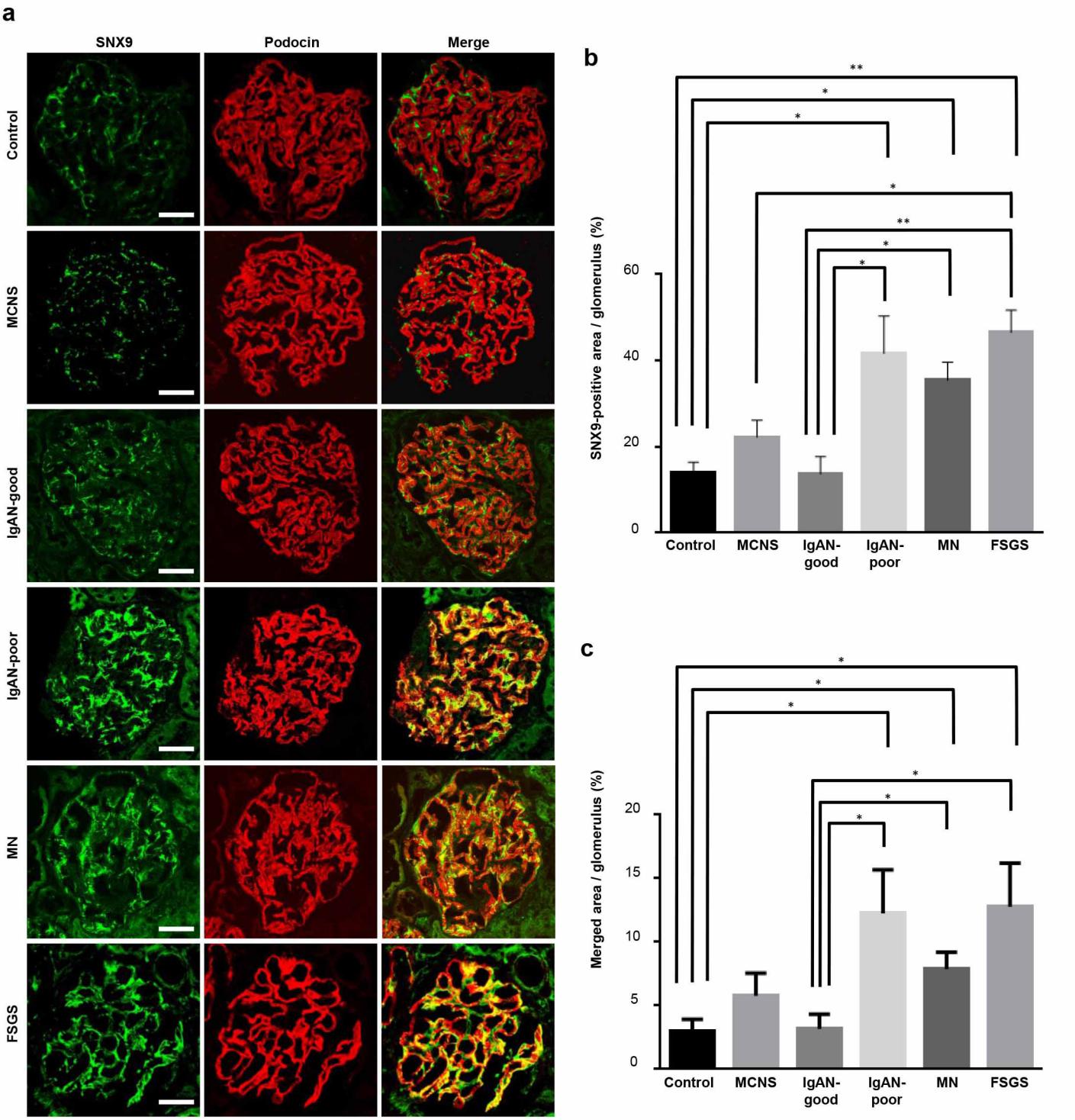
a
SNX9
Podocin
Merge
Control
MCNS
IgAN-good
IgAN-poor
MN
FSGS
b
SNX9-positive area / glomerulus (%)
0
20
40
60
Control
MCNS
IgAN-good
IgAN-poor
MN
FSGS
c
Merged area / glomerulus (%)
0
5
10
15
20
Control
MCNS
IgAN-good
IgAN-poor
MN
FSGS

Supplementary figure legends

Supplementary Figure S1. SNX9 is expressed in human cultured podocytes and glomeruli. To assess the distribution of SNX9, an antibody was raised against SNX9. Cultured human podocytes, mouse glomeruli and mouse kidneys were found to express SNX9 to different degrees. SNX9 was dominantly expressed in differentiated podocytes and glomeruli. Quantifications are presented as protein expression ratio normalized to β-actin. Mouse testis lysate was used as a positive control.

Supplementary Figure S1